

A Method for Studying Protein Orientation with Atomic Force Microscopy Using Relative Protein Volumes

Magnus Bergkvist,^{*,†} Jan Carlsson,[‡] and Sven Oscarsson[†]

Department of Chemical Engineering, Mälardalen University, Box 325, S-63105, Eskilstuna, Sweden, and Surface Biotechnology Center, Uppsala University, Box 577, S-75123, Uppsala, Sweden

Received: October 26, 2000; In Final Form: January 3, 2001

A method for studying protein orientation is described, in which the relative volumes of single proteins and single molecule complexes are measured using atomic force microscopy (AFM). Site-specific ligands are used as “probes” to bind to surface adsorbed proteins. The quantity of formed complexes gives an estimate of the amount of protein oriented in such a way as to allow ligand binding. The volume distribution for single proteins adsorbed to a surface was calculated and fitted to a Gaussian function. This volume distribution was used to localize the same proteins on surfaces with protein–ligand complexes, thus rendering it possible to find the amount of complex formed. Two model systems were used: one with two different mouse monoclonal antibodies of IgG1 type (mAb's against human serum transferrin, hST) adsorbed on silicon surfaces, and one with hST adsorbed to unmodified mica and aminated mica. The adsorbed proteins were allowed to react with a site-specific ligand, which binds to a defined region of the adsorbed protein (hST in the case of adsorbed mAb and lectin in the case of adsorbed hST). A great difference in ligand binding was found between the two antibodies adsorbed to the same type of surface as well as between hST adsorbed to different surfaces. This difference can be attributed to different orientation of the proteins on the surface. The general approach of this method suggests that it can be used for almost any site-specific molecule, either for surface orientation studies or studies where single molecule interactions need to be investigated.

Introduction

Protein behavior at solid–liquid interfaces is of great importance in nature, as such interactions play a fundamental role in the function and viability of living organisms. From a more practical point of view, many biotechnical and biomedical devices rely on the interaction between proteins and surfaces. Protein–surface interaction involves a number of physical properties such as charge, hydrophobicity, steric repulsion, etc., as well as kinetic properties. It is important to know how proteins interact, orient, and bind to various surfaces to be able to manufacture, for example, biocompatible materials for implantation and immunodiagnostic devices with high sensitivity and specificity.

In the past, orientation of proteins on surfaces has been investigated mainly by methods such as fluorescence spectroscopy, X-ray photoelectron spectroscopy (XPS), ellipsometry, surface plasmon resonance (SPR), and neutron reflectivity.^{1–9} The latter two techniques relate the orientation of molecules to an average value of the protein layer thickness. Recently, more powerful instrumentation with the ability to analyze individual molecules has been developed. One of these instruments is the atomic force microscope (AFM), which rapidly has become an essential tool in a wide variety of research fields. With the AFM it is possible to analyze individual protein molecules and their orientation/function on surfaces. This can be done by several approaches, for example, measurement of the protein height and comparison with its known dimensions (e.g., X-ray crystallography or NMR);¹⁰ examination of the protein “tilt” on the

surface;¹¹ or study the interaction of a “probe”-protein with a protein under investigation by detecting a height increase upon reaction.¹² Height measurements using AFM on single proteins has been used to probe molecular orientation but is sensitive to the protein shape. As an example, if one is interested in the orientation of a globular protein adsorbed to a surface, it is hard to find the right orientation just by height measurements, as all axes of the protein are similar. This problem can be solved if one uses a specific ligand (probe-molecule), which binds to a specific region of the protein of interest (target-molecule). In this study, we present a method for studying protein orientation by measuring the relative protein volume increase when a site-specific ligand protein binds to a target protein using tapping mode atomic force microscopy (TM-AFM). To evaluate the method we used two different model systems. First the orientation of monoclonal antibodies directed against human serum transferrin (hST), adsorbed to silica surfaces (Figure 1, schematic figure of immunoglobulin structure) was investigated using the hST as the probe-molecule.

Second, the orientation of hST adsorbed to unmodified and aminated mica surfaces was examined using *Sambucus nigra* (elderberry) bark lectin, which binds to a specific sugar residue in hST. These systems were chosen because the selected target and probe proteins can easily be obtained in pure and well-characterized form, for the interest in immunoglobulins in general and their great dependence on orientation for use in various applications. By reacting the probe-molecules with their respective target-molecule, measuring the volume of the formed protein complexes, and comparing to individual protein volume distributions, it is possible to calculate the amount of proteins that have an orientation in which their respective binding domains are accessible for binding.

* Author to whom correspondence should be addressed.

[†] Mälardalen University.

[‡] Uppsala University.

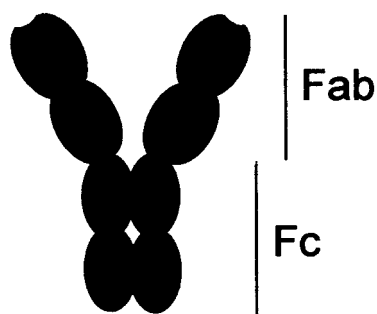


Figure 1. Schematic structure of IgG where Fab and Fc domains are marked.

Materials

Human serum transferrin (Sigma), ammonium acetate (Riedel-de-Haën), acetic acid (Merck), NaCl (Merck), elderberry (*Sambucus nigra*) bark lectin (Vector laboratories), human serum albumin (Sigma), galactose (Sigma), high-purity deionized water 18.2 Ω (MilliQ), 2 mouse IgG1 monoclonal antibodies directed against human serum transferrin (denoted mAb1 ($I_p = 6.3 \pm 0.2$) and mAb2 ($I_p = 5.9 \pm 0.2$)) (Pharmacia Diagnostica), General mouse IgG1 monoclonal antibodies (Pharmacia Diagnostica), 3-aminopropyltriethoxymethylsilane (ABCRC), n-doped silicon wafer, 3 Ω Cm (Wacker Siltronic), and muscovite ruby mica (Asheville-Schoonmaker Mica Co.) were used as received. All TM-AFM measurements were performed on a Digital Instrument Nanoscope IIIa Multi Mode AFM, using silicon tips (NM-TD) with an end radius of 5–10 nm, operated at a resonance frequency of approximately 100 kHz, and ~ 1 V free amplitude.

Methods

Surface Preparation. (a) *Silica.* The silica surfaces were cleaned in a piranha solution (2:1 $H_2SO_4:H_2O_2$) for 5 min and then sonicated 2 times for 5 min in ethanol, rinsed with water, and sonicated 2 times for 5 min in water. All surfaces were used immediately after cleaning.

(b) *Unmodified Mica.* The top layer of a mica surface was peeled off using scotch tape to make a fresh clean atomically flat surface

(c) *Aminated Mica.* A piece of mica was prepared as above. An amount of 100 μ L of 3-aminopropyltriethoxymethylsilane (APDES) was added to a quartz cuvette and the mica surface was placed on top and left to react under vacuum for 60 min. All surfaces were imaged before use and stored under vacuum if not used immediately after derivatization.

Contact angle measurements were performed on all surfaces with the sessile drop method according to Dahlgren.¹³

Protein Solutions. A rinsing buffer solution of 10 mM ammonium acetate in MilliQ water was prepared and pH adjusted to 7.0 with acetic acid if necessary. A similar buffer but with added 0.1 M NaCl was used for transferrin (hST) and immunoglobulin adsorption and 1 M NaCl for the lectin adsorption (adsorption buffer). Protein solutions of 2 and 4 μ g/mL (hST), 1.5 μ g/mL of each antibody, 2 and 4 μ g/mL of lectin, 2 and 4 μ g/mL of lectin with added 0.1 M galactose, and 1 μ g/mL of human serum albumin (HSA) were prepared in respective adsorption buffer.

Protein Adsorption. The adsorption of proteins to the surfaces was performed in a set of experiments as follows:

1. Three surfaces were placed in small flow cells with a volume of approximately 50 μ L. Adsorption buffer was added to wet the silica surface and then 50 μ L of the 1.5 μ g/mL

Bearing Analysis

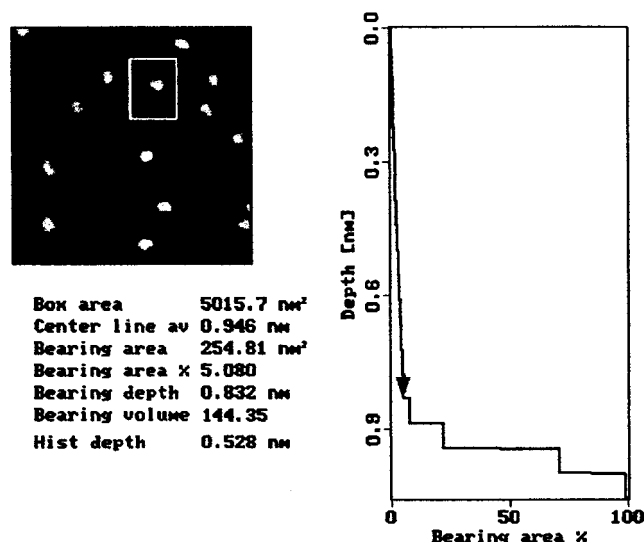


Figure 2. Bearing volume image where one hST molecule is analyzed.

immunoglobulin solution was added to two of the surfaces and protein adsorption was allowed to take place for 5 min. The third surface was exposed to adsorption buffer.

2. All three surfaces were rinsed with 2 mL of adsorption buffer before 50 μ L of the 2 μ g/mL hST solution was injected to one of the IgG surfaces and the surface without any preadsorbed protein. Adsorption and immuno-complex formation were permitted to take place for 5 min.

3. All surfaces were rinsed with 3 mL of rinsing buffer and dried with nitrogen and imaged in the AFM using the *same tip for all three surfaces in the experiment set.*

The same procedure was performed for all immunoglobulins and concentrations of hST.

This yields three surfaces: one with adsorbed IgG, one with possible immuno-complexes and one surface with adsorbed hST.

The same protocol was followed for adsorption of 2 μ g/mL of hST with subsequent lectin addition (with and without added galactose) and for HSA adsorption with following lectin addition, but with the difference that the surfaces were dried and imaged after the washing in step 2 before continuing addition of protein or buffer.

Experiments in which one monoclonal antibody was adsorbed to three different silica surfaces using the above procedure, without the hST addition were used as a reference to show that the volume distribution for a certain protein species is the same when using the same tip.

Measurements. Images of 1 μ m² scan size were recorded and volumes and heights of the adsorbed molecules were analyzed, using the bearing-analysis feature in the nanoscope software (Figure 2). A normal distribution of volumes was calculated with a bin size of 25 nm³. A Gaussian equation was fitted to the volume distribution on the surfaces with adsorbed single molecule species and the resulting function was used to find the corresponding molecule distribution on the surface with both proteins present. By keeping the peak center and full width of half-maximum from the single protein volume distributions and fitting the Gaussian function to the volume distribution peaks on the surface with protein complexes, it was possible to determine the amount of overlap of the protein distributions and the amount of each protein species on the surface (see Figures 3–4b, Table 3).

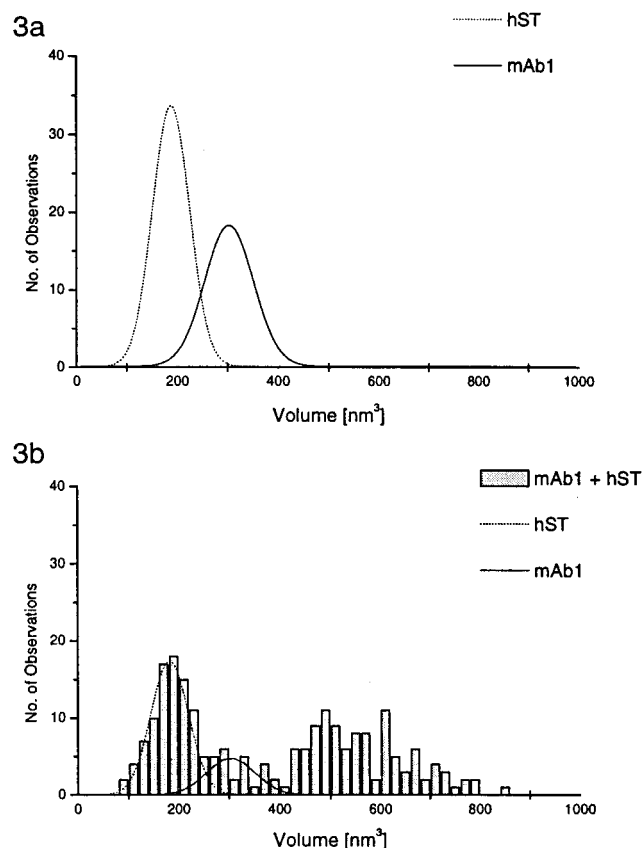


Figure 3. (a) Gaussian fit to the volume distribution for mAb1 and hST adsorbed to separate silica surfaces. (b) Volume distribution for mAb1 and hST adsorbed to the same silica surface where each protein's Gaussian function is fitted to the histogram.

Results

To minimize the risk for sterical hindrances of the antigen/lectin binding due to unspecific protein–protein interactions a surface coverage $<0.5\%$ for all surfaces were used. The amount of mAb adsorbed to the silica surfaces was approximately 100 molecules/ μm^2 . The amount of adsorbed hST to silica from the 2 $\mu\text{g/mL}$ solution was approximately 100 molecules/ μm^2 and 200 molecules/ μm^2 for the 4 $\mu\text{g/mL}$ solution. On unmodified and aminated mica, the adsorption of hST was between 60 and 90 molecules/ μm^2 while lectin essentially did not adsorb to the surfaces except for a few molecules. A minimum of three sets of experiments were performed for each protein–ligand system. The results presented are from *one* set of experiments rather than the averaged values from the three sets performed (see Discussion). An amount of 80–90% of the adsorbed hST had an apparent elliptical shape on both mica and aminated mica and $>95\%$ of the IgG molecules a circular shape, as revealed by AFM. Contact angle measurements on the surfaces were made according to Dahlgren.¹³ The values found were similar for silica and unmodified mica, i.e., $0-7^\circ$, while the aminate mica was more hydrophobic with a contact angle of $50-55^\circ$.

Docking Experiments with hST to Preadsorbed mAb1.

The volume distribution for mAb1 adsorbed to silica revealed a peak at $309 \pm 61 \text{ nm}^3$, hST adsorbed to silica showed a volume distribution of $190 \pm 55 \text{ nm}^3$ (Figure 3a, Gaussian function, Table 1). When measuring the volume distribution on the surfaces where hST was added to preadsorbed mAb1, the volume distribution curve was partly shifted to higher volumes. At the same time, the peak corresponding to the original mAb1 population was reduced (Figure 3b). A mean value for the new

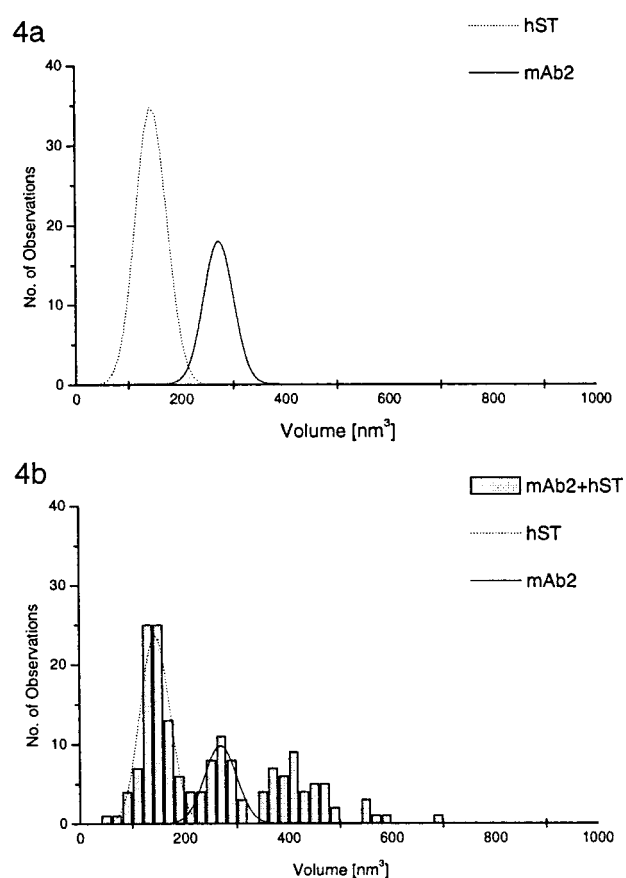


Figure 4. (a) Gaussian fit to the volume distribution for mAb2 and hST adsorbed to separate silica surfaces. (b) Volume distribution for mAb2 and hST adsorbed to the same silica surface where each protein's Gaussian function is fitted to the histogram.

TABLE 1: Mean Volume Distribution for mAb1, mAb2, hST, and mAb + hST Complexes for One Experiment Set

protein	volume [nm ³]	protein	volume [nm ³]
mAb1	309 ± 61	mAb2	291 ± 58
hST	190 ± 55	hST	142 ± 56
mAb1 + hST	487 (first peak)	mAb2 + hST	411 ± 42

TABLE 2: Mean Volume Distribution for hST, hST + Lectin Complexes, hST + Lectin with Added Galactose for One Experiment Set

protein	unmodified mica [nm ³]	aminated mica [nm ³]
hST	148 ± 21.5	143 ± 21.5
hST + lectin	388 ± 78.5	393 ± 85.5
hST + lectin/Gal	146 ± 19.5	144 ± 22.5

volume peak of mAb1–hST complexes is difficult to give, as it is clear from the distribution that there is more than one population present, possibly from binding of two hST to one mAb1, with one population centered around 487 nm^3 . When calculating the amount of reacted mAb1, using the Gaussian functions obtained from the surfaces with single molecule species adsorbed, it was found that $\sim 80\%$ of the mAb1 were able to bind hST (Table 3).

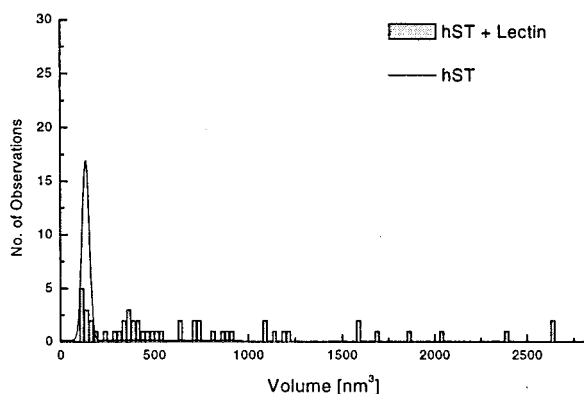
Docking Experiments with hST to Preadsorbed mAb2.

The volume distribution of mAb2 adsorbed to silica resulted in a peak at $291 \pm 58 \text{ nm}^3$, hST adsorbed to silica gave a peak at $142 \pm 56 \text{ nm}^3$ (Figure 4a, Gaussian function, Table 1). When hST was added to the mAb2 adsorbed on silica, a volume distribution at $411 \pm 42 \text{ nm}^3$ appeared (Figure 4b, Table 1). Measuring the volume distribution for the surface with adsorbed mAb2 with added hST, using the their respective Gaussian

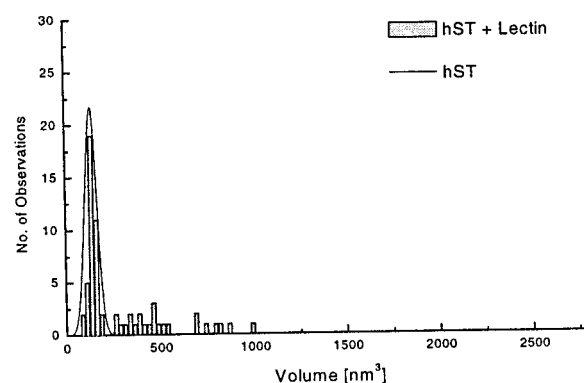
TABLE 3: Amount of Complex Formation, for mAb and hST with Corresponding Ligand. Free Protein Is the Amount of mAb and hST that Has Not Reacted with Their Corresponding Ligand

	mAb1 + hST silica	mAb2 + hST silica	hST + lectin mica	hST + lectin aminated mica	hST + lectin 0.1 M Gal all surfaces
protein complex	80%	50%	80%	40%	0%
free protein	20%	50%	20%	60%	100%

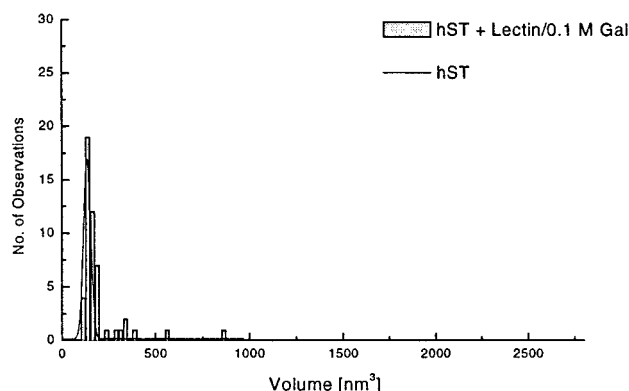
5a



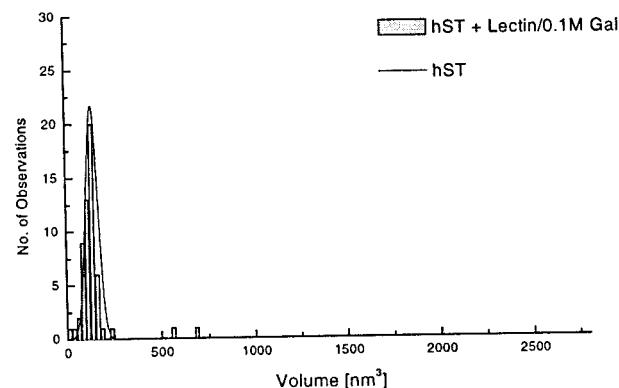
6a



5b



6b

**Figure 5.** (a) Volume distribution for hST and hST + lectin adsorbed to the same mica surface. Gaussian function of hST is included to visualize the hST peak (solid line). (b) Same as above but with 0.1 M galactose added to the lectin solution.

functions to find the percentages of each molecule species, it was found that $\sim 50\%$ of the mAb2 had reacted with hST (Table 3).

Docking of hST to mAb1 and mAb2 at Higher Concentrations. When using the double concentration of hST ($4\mu\text{g}/\text{mL}$), no difference from the above results were found, except for a higher unspecific binding of hST to the silica surface (data not shown).

When using monoclonal immunoglobulins without any specificity for hST, no volume shift for the mAb distribution was observed and the populations for the two proteins were the same as on the surfaces with just single protein species adsorbed (data not shown).

Docking Experiments of Lectin to Preadsorbed hST on Unmodified Mica Surfaces. The volume distribution for transferrin on mica revealed a peak at $148 \pm 21.5 \text{ nm}^3$. When lectin was added, $\sim 80\%$ of the initial transferrin volume distribution peak was spread out over a wide range, but with a part of the population at $388 \pm 78.5 \text{ nm}^3$ (Figure 5a, Table 2). When 0.1 M galactose was added to the lectin solution, the volume shift was not observed and the volume distribution was similar to that of adsorbed transferrin alone (Figure 5b, Table 2). Thus 80% of the hST is able to bind lectin (Table 3).

Figure 6. (a) Volume distribution for hST and hST + lectin adsorbed to the same aminated mica surface. Gaussian function of hST is included to visualize the hST peak (solid line). (b) Same as above but with 0.1 M galactose added to the lectin solution.

Docking Experiments of Lectin to Preadsorbed hST on Aminated Mica Surfaces. Transferrin adsorbed to aminated mica surfaces gave a volume distribution at $143 \pm 21.5 \text{ nm}^3$. After the addition of lectin to the adsorbed transferrin, a new population was observed at $393 \pm 85.5 \text{ nm}^3$, which corresponds to 30% of the total amount of adsorbed proteins plus some larger complexes, corresponding to 10% of the total amount (Figure 6a, Table 2). The initial transferrin peak at 143 nm^3 decreased by 40% compared to the same surface before addition of lectin (the increased complex formation equals the loss of single hST). If lectin that had been pretreated with 0.1 M galactose was added to the surface with preadsorbed transferrin, the population at 393 nm^3 and the larger complexes were not present. The original transferrin peak did not change when adding lectin but was the same as for a single population of hST (Figure 6b, Table 2). The complex formation of lectin to hST corresponds to 40% (Table 3).

Docking Experiments of Lectin to HSA on Mica Surfaces. As a control for unspecific protein binding, lectin was added to mica with preadsorbed HSA, a protein that does not contain any carbohydrate moiety. No binding was observed (data not shown), which indicates that unspecific protein binding in the experiment is not responsible for the formation of transferrin/lectin complexes.

TABLE 4: Volume Increase of mAb Complex, and Standard Error of Protein Populations

5 ^a	volume increase of complex relative to mAb (%)	5 ^b	standard error for protein populations—different AFM tips (%)	standard error for protein populations—same AFM tip (%)
mAb1	38 ± 2	mAb1	13	3.25
mAb2	36 ± 5	mAb2	27	
		hST	15	

^a Volume increase in percent when mAb forms complex with hST, calculated as $(V_{\text{complex}} - V_{\text{mAb}})/V_{\text{complex}}$. Average value calculated from three experiment sets for each one of the two mAb's. ^b Standard error of the mean volume for three experiments on mAb1, mAb2, and hST, respectively, adsorbed to silica where different AFM tips were used for each experiment, compared to the standard error of three experiments of adsorbed mAb1 obtained with the same AFM tip. As the table illustrates, the standard error can be substantial when different tips are used to scan the same protein population.

To make sure that the variations in experimental setups, such as sample thickness, tip-wearing, and local tip—surface interactions between different surfaces did not affect the volume measurements when using the same tip, a control experiment was performed in which three silica surfaces with adsorbed mAb were imaged using the same tip to investigate whether results are repeatable. It was found that for the three surfaces scanned, the standard error was 3.25% for over 300 scanned proteins. Experiments carried out with different tips showed standard errors of almost 30% (Table 4b).

Discussion

Atomic force microscopy (AFM) has recently been introduced in biological science as a tool for studying protein structure¹⁴ and protein activity.¹⁵ It has also been used for measuring mechanistic properties of proteins and DNA.^{16–19} In these kinds of work AFM is used for its excellent force measuring capabilities rather than its imaging qualities. Schneider et al.²⁰ measured the height and diameter of a protein and calculated the volume by treating the molecule as a segment of a sphere, showing that there is almost a linear relationship between the molecular weight and the volume of proteins measured with AFM. In this study, we used the imaging capabilities of AFM to measure relative protein volumes. Using this procedure, we can distinguish between different proteins and see if protein complexes are formed. By using a specific “probe” protein, which binds to a specific region of the protein under investigation, it is possible to get information about the orientation of the adsorbed “target” protein. Instead of calculating the volume of a sphere, which could be troublesome, as we do not know the exact shape of the complex formed, we use the bearing volume feature in the nanoscope software, which calculates the volume of pixels above a threshold level (Figure 2). The obtained data give the opportunity to calculate volumes of proteins and complexes, which give qualitative information of orientation of single molecules, as well as quantitative information on populations of molecules/complexes on different surfaces. The measured volume is not necessarily the correct volume of the proteins, but as we are interested in measuring relative differences in volume, this fact is of minor importance. To ensure that use of the same tip give reproducible volume measurements, an experiment with mAb1 adsorbed to three silica surfaces was made, and it was found that the mean volume for IgG on these surface had a standard error of 3.25% between the means for the three surfaces (Table 4).

Orientation of mAb's on Silica Surfaces. Immunoglobulins are well-known proteins with a characteristic structure where the binding of antigen (in this case hST) occurs at the end of the so-called Fab domain, which makes the protein complex formation very site-specific (Figure 1). Results from the binding of hST to surfaces with different adsorbed mouse IgG1 monoclonal antibodies (denoted mAb1 and mAb2), show that

there is a major difference of antigen binding for the two antibodies (Figure 3b and 4b). mAb1 binds approximately 80% of the hST while mAb2 binds only 50% of hST (Table 3). This difference clearly indicates a preferential orientation for mAb1 with the Fab domains protruding from the surface while mAb2 has an orientation with a less exposed Fab domain. The different orientations obtained for the two antibodies is not that surprising since monoclonal antibodies could have significant differences in their physical properties, i.e., varying isoelectric point, hydrophobicity, etc., leading to different stability.²¹ It has been discussed in the literature that the Fc domain of IgG adsorbs to negatively charged silica surfaces, especially with low surface coverage, depending on its relatively low structural stability.⁵ The low stability for the Fc domain and its importance for oriented adsorption has been shown in a study by Andrade et al.,^{22,23} in which antibodies adsorbed to polystyrene surfaces increased their antigen binding as a result of pretreatment at acidic pH. This was explained by an unfolding of the Fc domain, which increased preferential binding of this domain to the surface. It may well be that the Fc domain in mAb1 is more likely to unfold than the Fc domain in mAb2, thus adsorbing the mAb1 in a more end-on orientation. Reduced binding of antigen as a result of unfolding of the Fab domains in mAb2 is less likely as these domains are considered to be quite stable toward unfolding.^{5,24,25} Another possible explanation for different adsorption behavior of monoclonal antibodies could be differences in isoelectric point (Ip) leading to different net charges.²⁴ In our case, the Ip of mAb1 (6.3) and mAb2 (5.9) differs by merely 0.4 pH units so the effect of different charge should be minimal. But, there could of course be a local patch of charges not reflected by the isoelectric point, which cause the orientations. The most likely reason for the difference in orientation is a combination of structural stability of the Fc domain and local charge distributions. Side-on adsorption, where IgG is adsorbed flat on the surface seems unlikely as 95% of the proteins showed a circular shape and not the characteristic Y-shape of immunoglobulin, which has occasionally been imaged with AFM.¹²

Orientation of Transferrin on Unmodified and Aminated Mica Surfaces. Transferrin is a single chain protein with two lobes (Figure 7) ($21 \times 25 \times 35$ Å each lobe) with an elliptical shape. This elliptical shape can be seen in the AFM images on both mica and aminated mica, in which 80–90% of the hST molecules have an elliptical form indicating that they are adsorbed with their major axis horizontal to the surface. This is the most probable orientation for transferrin at low surface coverage.²⁶ hST contains a carbohydrate moiety, containing two branched sugar residues ending with negatively charged sialic acid groups at neutral pH, located in the C-terminal lobe (Figure 7). The *Sambucus nigra* lectin reacts specifically with terminal galactosyl-sialic acids, but can be inhibited with high concentra-

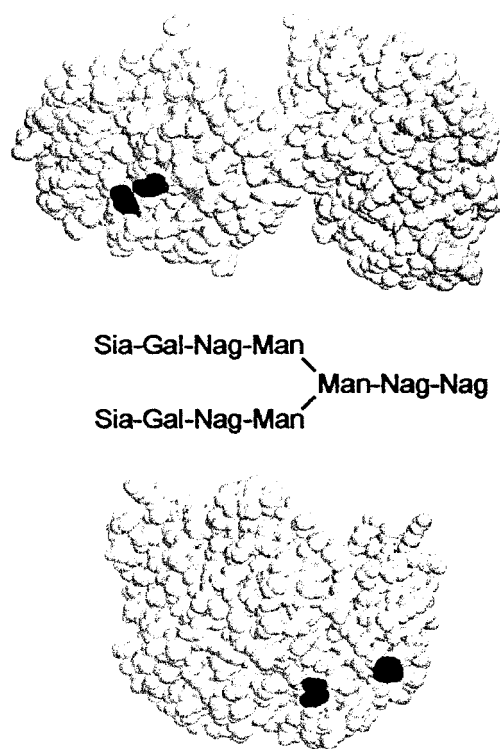


Figure 7. Theoretical structure of human serum transferrin (hST). The sugar sequence of one carbohydrate residue is shown and the locations of the carbohydrates in hST are marked with black, side and front view.

tions of galactose. This makes this lectin a perfect site-specific probe molecule for hST.

Unmodified Mica Surfaces. The mica surface is a hydrophilic surface with a minor negative charge (-0.0025 C/m^2 according to Pashley²⁷). Interactions between the protein and surface are likely to be mainly of electrostatic nature. As the carbohydrate residues in hST are located in one of the lobes, this part must be oriented away from the surface to be able to react with the lectin molecules. When galactose is present, it competes with the binding of hST galactosyl-sialic acids groups so that the biospecific interaction between transferrin and lectin is inhibited. On mica, transferrin generates a single peak in the volume distribution. When lectin is added to the transferrin adsorbed on mica, 80% of the hST population reacts to form complexes with lectin in the form of large aggregates, with a small population at 388 nm^3 (Figure 5a, Table 3). In comparison, addition of lectin to the reference surface gave no significant protein adsorption at all, showing that background adsorption on the mica surface is negligible. The high degree of complex formation, which can be seen as a large volume distribution shift, was followed by a similar decrease in the number of single transferrin molecules (80%), indicating that the sugar chains were accessible for binding. Another indication that there is a lectin–transferrin specific interaction is that the complex formation did not occur when galactose was present, resulting in a volume distribution similar to a single hST population. The complex formation with lectin and the shape of hST on the surface suggests that hST was adsorbed to mica in a side-on orientation with the carbohydrate chains exposed to the liquid phase (Figure 8a).

Aminated Mica Surfaces. The aminated mica surface is a positively charged, amphiphilic surface with a contact angle of $\sim 50^\circ$, so both hydrophobic and electrostatic interactions are likely to occur. Surface properties for aminated mica surfaces prepared with silanol reagents have been characterized by

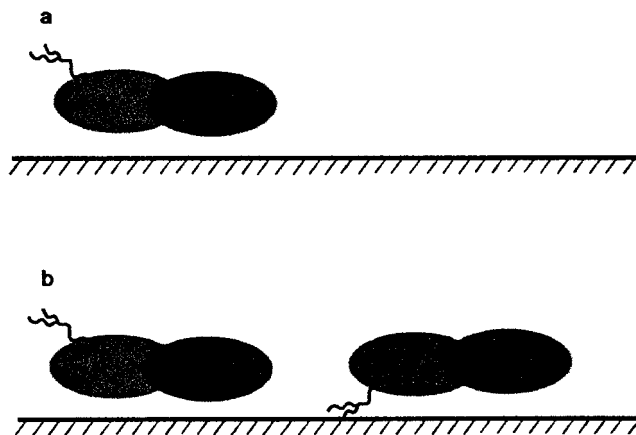


Figure 8. Schematic model showing possible orientations for hST on (a) unmodified mica and (b) aminated mica.

Lyubchenko et al.^{28–30} Upon addition of lectin to preadsorbed transferrin on aminated mica surfaces, a new population was formed as compared to a surface containing only transferrin (Figure 6a), where the distribution of volumes was not as pronounced as on the mica surface. The amount of complex corresponds to approximately 40% of the total amount of protein adsorbed (Table 3). The lectin reference surface adsorbed practically no lectin at all. As 40% of the total amount of protein on the surface was capable of binding lectin, this suggests two populations—one oriented in a side-on orientation in which the carbohydrate chain residues are accessible to binding (40%), and one population with a side-on orientation in which none of the carbohydrate residues are accessible for lectin binding (60%) (Figure 8b). The decrease in complex formation on aminated mica compared to unmodified mica may be due to a different attraction between polar/apolar groups in the amino acid side chains and/or negative sialic acids in the carbohydrate moiety toward the aminated surface. This interaction might orient one side of the C-terminal lobe of transferrin toward the surface, thus hiding the sugar moieties and reducing the lectin binding possibilities. An alternative explanation could be that an altered conformation of transferrin upon adsorption to the amphiphilic, aminated surface makes the carbohydrate residues inaccessible for lectin binding. Preliminary AFM studies of hST adsorbed to methylated mica surfaces with a similar hydrophobicity, as judged from contact angle measurements, showed that there is a clearly visible unfolding of hST not seen on the aminated mica surface. This indicates that the conformational change of hST on the aminated surface is considerably smaller than on the methylated mica surface.

The large variation in volumes for transferrin–lectin complexes on mica compared to the aminated mica surface, may be due to the fact that hST has four possible binding sites and thus can bind more than one ligand if all sites are available. Another explanation may be that transferrin has a higher lateral mobility on mica than on the other surfaces due to weaker interactions and a smaller probability of multipoint attachment which would occur on highly charged or hydrophobic surfaces, especially at low concentrations.^{31–34} As the *Sambucus nigra* lectin can bind more than one ligand,³⁵ polymerization or aggregation are possible if transferrin can move laterally on the surface. This would increase the apparent volume of the molecular complexes.

When using molecule–complex formation as a way to probe orientation, it is important that the binding of probe–molecule to target molecule reaches saturation. This is depending on the

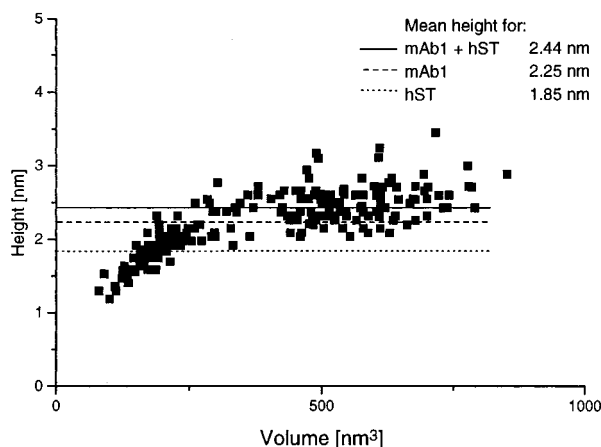


Figure 9. Volume vs height plot for mAb1 with added hST where the mean height for each population is marked. Notice the minimal height change compared to the large volume changes.

binding constant of the probe molecule. In our case, the binding constants are in the order of 10^3 – 10^5 M^{-1} for lectins³⁶ and 10^4 M^{-1} for both antibodies. A low binding of antigen or lectin, depending on preferential orientation of the target-molecule upon adsorption, may be mistaken for a nonsaturated binding. In this study, increased concentration of probe-molecules produced the same results as the lower concentration used, indicating that saturation was reached and reduced binding of lectin/hST to respective target-molecule is not due to low amounts of protein. Also, it is important to recognize that at these small surface concentrations of mAb and hST, there is a large excess of antigen/lectin in solution so depletion is unlikely. This, combined with a rinsing step and subsequent drying of the sample, ensured that little or no dissociation of immunocomplexes occur. To confirm that binding of hST to mAb1 and mAb2 were due to specificity of the antigen, mouse monoclonal IgG1 without specificity for hST were used as a control, and no immunocomplex formation was observed. A similar verification was performed for the lectin, in which surface adsorbed HSA, devoid of carbohydrate moieties, was exposed to the lectin solution and no binding was found. This, combined with the fact that galactose inhibited the lectin binding to hST, strongly indicates that the binding of lectin to hST is specific.

Assessment of the Method. As can be seen from the results, this method of using relative volumes clearly reveals whether molecular complexes are formed or not. Comparing the use of protein volumes to protein heights for detecting molecular complex formation, an approach used in the pioneering work by Quist et al.,¹² where polyclonal antibodies against albumin were used, it is not necessarily true that the height would change significantly. This is especially important when using a site-specific probe molecule that, depending on orientation of the target molecule, does not necessarily react on top of it. Another difficulty is if the probe molecule in itself adsorbs to the surface after binding, producing minimal height change. In both these cases, a volume increase would be detected. An example of this can be seen in Figure 9, where height vs volume for mAb1 and hST is shown. The height change when hST bind mAb1 is minimal compared to the large volume shift. As volume measurement is related to mass, a few limits are put on this kind of systems. The target protein must have enough mass/volume, as to be measured by AFM, and the probe protein, which is supposed to react on the target molecule, must add sufficient mass/volume to be able to measure the increased size of the molecular complex. In the IgG experiment, molecular weights of 80 kD (hST) and 150 kD (IgG) were used, resulting

in a molecular complex with a molecular weight of approximately 230 kD, i.e., approximately a mass increase of 35% relative the mass of a IgG molecule.

One reason for the lack of use of the AFMs imaging strengths on biological system on single protein level, is the problem of giving the correct dimensions for a protein molecule. As the tip curvature have a high impact on the shape on imaged objects in the same scale as the AFM tip, tip-induced artifacts result in an overestimation of the object size.^{37,38} This can be adjusted for if the tip shape is deconvoluted and the image reconstructed to give a more accurate dimension of the observed objects.³⁹ This can be rather troublesome and it may still not be the right protein dimension and height that is measured, as the tip can deform the molecule while scanning. This problem is, however, of minor importance when measuring relative protein volumes as it is the increase of volume that is interesting. The only experimental parameter of importance, is that the volume distributions of the proteins used is measured using the same tip, as different tips can give shifts in volume distributions depending on tip shape, laser position on the cantilever, tip surface interactions, etc. Standard errors as large as 30% of the mean volumes have been measured with different AFM tips, whereas using the same tip give standard errors of only 3.25% (Table 4). Even though there can be large volume shifts between experiment sets when different AFM tips are used, the relative increase in volumes when complex is formed is constant between the experiment sets. An example is shown in Table 4 where the volume increase of mAb–hST complexes relative to mAb is 36–38% which is very close to the predicted mass increase of the complex, i.e., 35%.

With the development of higher aspect ratio tips with smaller tip curvature, for example, single-walled nanotube tips, it would be possible to measure more accurate protein volumes and thus increase the resolution of this method. The straightforward approach of this technique makes it possible to use all kinds of specific probe molecules and a variety of surfaces for work where molecular complexes needs to be detected at the single molecule level, for example orientation studies.

Conclusion

The results presented in this manuscript show the possibility of getting detailed information about the orientation of a protein molecule on a surface by determination of the relative volume increase of a protein before and after a biospecific interaction. The orientations of two kinds of monoclonal antibodies against transferrin were examined with AFM on native silicon wafers. The orientation of transferrin itself was investigated on mica and chemically derivatized mica by use of a biospecific lectin against the carbohydrate moieties in the transferrin molecule. The two different monoclonal antibodies were oriented in such a way that 80% and 50%, respectively, could react with their antigen. The transferrin molecules were oriented in such a way that the carbohydrates were able to bind >80% of lectin on native mica and 40% on aminoderivatized mica. The reliability of the method is high, if the same tip was used a correlation coefficient of 3.25% was obtained, which shows that the technique is powerful with possibilities to get a direct evaluation of the orientation of macromolecules on different kinds of surfaces.

Acknowledgment. We thank Dr. J. Buijs, Dr. A. Quist, and Dr. S. Dunne for proofreading the manuscript and for valuable discussions. This work was founded by the Swedish Ministry of Education and the KK-Foundation.

References and Notes

- (1) Kowalczyk, D.; Slomkowski, S. *J. Bioact. Comput. Pol.* **1994**, *9*, 282–308.
- (2) Söderquist, M. E.; Walton, A. G. *J. Colloid Interface Sci.* **1980**, *75*, 387–397.
- (3) Ivarsson, B. A.; Hegg, P. O.; Lundström, I.; Jönsson, U. *J. Colloid Interface Sci.* **1985**, *13*, 169–192.
- (4) Jönsson, U.; Lundström, I.; Rönnberg, I. *J. Colloid Interface Sci.* **1987**, *117*, 127–138.
- (5) Buijs, J.; Norde, W.; Lichtenbelt, J. W. T. *Langmuir* **1996**, *12*, 1605–1613.
- (6) Malmsten, M. *Colloid Surf. B: Biointerfaces* **1995**, *3*, 297.
- (7) Vasques, R. P.; Margalit, R. *Thin Solid Films* **1990**, *192*, 173–180.
- (8) Su, T. J.; Lu, J. R.; Thomas, R. K.; Cui, Z. F.; Penfold, J. *Langmuir* **1998**, *14*, 438–445.
- (9) Lu, J. R.; Su, T. J.; Thirtle, P. N.; Thomas, R. K.; Rennie, A. R.; Cubitt, R. *J. Colloid Interface Sci.* **1998**, *206*, 212–223.
- (10) Waner, M. J.; Gilchrist, M.; Schindler, M.; Dantus, M. *J. Phys. Chem. B* **1998**, *102*, 1649–1657.
- (11) Bergkvist, M.; Carlsson, J.; Oscarsson, S. *J. Colloid Interface Sci.* **1998**, *206*, 475–481.
- (12) Quist, A. P.; Bergman, A.; Reimann, C.; Oscarsson, S.; Sundqvist, B. *Scanning Microsc.* **1995**, *9*, 395–400.
- (13) Dahlgren, C.; Sundqvist, T. *J. Immunol. Methods* **1981**, *40*, 171–179.
- (14) Möller, C.; Allen, M.; Elings, V.; Engel, A.; Müller, D. *J. Biophys. J.* **1999**, *77*, 1150–1158.
- (15) Radmacher, M.; Fritz, M.; Hansma, H. G.; Hansma, P. K. *Science* **1994**, *265*, 1577–1579.
- (16) Florin, E. L.; Moy, V. T.; Gaub, H. E. *Science* **1994**, *262*, 415–417.
- (17) Hinterdorfer, P.; Schilcher, K.; Baumgartner, W.; Gruber, H. J.; Schindler, H. *Nanobiology* **1998**, *4*, 177–188.
- (18) Sagvolden, G.; Giaever, I.; Feder, J. *Langmuir* **1998**, *14*, 5984–5987.
- (19) Trabesinger, W.; Schütz, G. J.; Gruber, H. J.; Schindler, H.; Schmidt, T. *Anal. Chem.* **1999**, *71*, 279–283.
- (20) Schneider, S. W.; Lärmer, J.; Henderson, R. M.; Oberleithner, H. *Eur. J. Physiol.* **1998**, *435*, 362–367.
- (21) Buijs, J.; Lichtenbelt, J. W. T.; Norde, W.; Lyklema, J. *Colloids Surf. B: Biointerfaces* **1995**, *5*, 11–23.
- (22) Lin, J. N.; Andrade, J. D.; Chang, I. N. *J. Immunol. Methods* **1989**, *125*, 67–77.
- (23) Chang, I.-N.; Lin, J.-N.; Andrade, J. D.; Herron, J. N. *J. Colloid Interface Sci.* **1995**, *174*, 10–23.
- (24) Buijs, J.; Van de Berg, P. A. W.; Lichtenbelt, J. W. T.; Norde, W.; Lyklema, J. *J. Colloid Interface Sci.* **1996**, *178*, 594–605.
- (25) Kawaguchi, H.; Sakamoto, K.; Ohtsuka, Y.; Ohtake, T.; Sekiguchi, H.; Iri, H. *Biomaterials* **1989**, *10*, 225–229.
- (26) Guemouri, L.; Ogier, J.; Ramsden, J. J. *J. Chem. Phys.* **1998**, *109*, 3265–3268.
- (27) Pashley, R. M. *J. Colloid Interface Sci.* **1981**, *83*, 531–546.
- (28) Lyubchenko, Y. L.; Oden, P. I.; Lampner, D.; Lindsay, S. M.; Dunker, K. A. *Nucleic Acids Res.* **1993**, *21*, 1117–1123.
- (29) Lyubchenko, Y. L.; Gall, A. A.; Shlyakhtenko, L. S.; Lindsay, S. M. *Biophys. J.* **1996**, *70*, WAMG6-WAMG6.
- (30) Shlyakhtenko, L. S.; Gall, A. A.; Weimer, J. J.; Hawn, D. D.; Lyubchenko, Y. L. *Biophys. J.* **1999**, *77*, 568–576.
- (31) Norde, W. *Cells Mater.* **1995**, *5*, 97–11–2.
- (32) Tilton, R. D.; Gast, A. P.; Robertson, C. R. *Biophys. J.* **1990**, *58*, 1321–1325.
- (33) Yang, Z.; Galloway, J. A.; Yu, H. *Langmuir* **1999**, *15*, 8405–8411.
- (34) Buijs, J.; Hlady, V. *J. Colloid Interface Sci.* **1997**, *190*, 171–181.
- (35) Van Damme, J. M.; Barre, A.; Rougé, P.; Van Leuven, F.; Peumans, W. *J. Eur. J. Biochem.* **1996**, *235*, 128–137.
- (36) Fasman, G. D. *Handbook of Biochemistry and Molecular Biology Proteins*; CRC Press: Boca Raton, FL, 1986; Vol. 2.
- (37) Ramirez-Aguilar, K. A.; Rowlen, K. L. *Langmuir* **1998**, *14*, 2562–2566.
- (38) Howald, L.; Haefke, H.; Luthi, R.; Meyer, E.; Gerth, G.; Rudin, H.; Guntherodt, H. *J. Phys. Rev. B: Condens. Matter* **1994**, *49*, 5651–5656.
- (39) Markiewicz, P.; Goh, M. C. *Langmuir* **1994**, *10*, 5–7.